ELSEVIER

International Journal of Mass Spectrometry 189 (1999) 147–156

International Journal of Mass Spectrometry

Formation of lead/sulfur binary cluster ions by laser ablation

Jian-bo Liu, Chun-ying Han, Wei-jun Zheng, Zhen Gao*, Qi-he Zhu

State Key Laboratory of Molecular Reaction Dynamics, Institute of Chemistry, Chinese Academy of Sciences, Beijing 100080, People's Republic of China

Received 1 November 1998; accepted 14 April 1999

Abstract

Lead/sulfur binary cluster ions were produced by laser single ablation and laser double ablation, respectively, photolyzed by a UV laser and detected with a tandem time-of-flight (TOF) mass spectrometer. The distribution of cluster ions produced by laser single ablation is different from that produced by laser double ablation. By laser single ablation on a mixed Pb + S target, $Pb_nS_{n-1}^+$ and $Pb_nS_n^-$ are formed as stable compositions that serve as structural skeletons of the binary clusters. All other cluster ions can be indicated as $Pb_nS_m^+$ with $m \geq n - 1$ or $Pb_nS_m^-$ with $m \geq n$, produced by the attachment of excess S atoms to $Pb_nS_{n-1}^+$ or $Pb_nS_n^-$. The stable compositions shown above are also found in the fragments from the main photodissociation channels of cluster cations, confirming their special stability. The structural models of the cluster ions with stable compositions are proposed. On the other hand, by laser double ablation on a separated Pb target and S target, the Pb clusters and S clusters are formed independently and then react with each other to generate binary cluster ions $Pb_nS_m^+$ and $Pb_nS_m^-$ with $n = 1$–7 and $m \geq 0$. These two different formation pathways, by laser single ablation and laser double ablation, respectively, can lead to distinct differences in the compositions and distributions of the cluster ions. The different properties, such as internal energies or structural isomers, for a single stoichiometry from the different formation pathways are also discussed. (Int J Mass Spectrom 189 (1999) 147–156) © 1999 Elsevier Science B.V.

Keywords: Lead/sulfur clusters; Laser ablation; Time-of-flight (TOF) mass spectrometer; Photodissociation

1. Introduction

Lead sulfide compound (PbS) has been well known as a *p*-type semiconductor that is sulfur rich and an *n*-type semiconductor that is lead rich [1]. Recently, the Pb/S cluster has drawn much more interest than bulk PbS and has become the focus of semiconductor cluster studies [2,3]. In comparison with bulk PbS, the Pb/S cluster shows a large blue shift of the absorption edge. The bandgap of the cluster shifts from the infrared region of bulk compound to the visible region [4], which is quite valuable for electroluminescent devices such as light-emitting diodes. In addition, the Pb/S cluster is expected to have exceptional third-order nonlinear optical properties [5], and may also be useful in optical devices such as optical switches.

Pb/S nanoclusters have been synthesized in the condensed phase by reaction of Pb^{2+} with H_2S in the porous matrices such as zeolites [6], ionomers films [4], and copolymer nanoreactors [7]. The isolated Pb/S binary clusters have also been produced in the gas phase by adiabatic cooling of the vapor of the PbS compound [8,9]. By these preparation methods, the 1:1 stoichiometry of Pb and S was maintained

* Corresponding author. E-mail: gaoz@mrdlab.icas.ac.cn

1387-3806/99/$20.00 © 1999 Elsevier Science B.V. All rights reserved
PII S1387-3806(99)00068-8

throughout the cluster growth. As a result, the clusters with stoichiometric compositions like $(PbS)_n$ were mainly produced, whereas the clusters with non-stoichiometric compositions were difficult to obtain. However, in view of the transition of matter from atoms or molecules to the condensed phase, the experimental study on Pb/S binary clusters with all possible compositions as well as the nonstoichiometric–stoichiometric composition transition is a more important aspect of Pb/S cluster studies. With this in mind, we used the technique of laser ablation to produce Pb/S binary cluster ions in the gas phase. The laser ablation with a single laser beam can accomplish the vaporization and ionization of the sample, followed by the clustering process [10]. During the laser-based clustering process, the produced clusters are subjected to frequent collisions with each other, which can lead clusters to dissociation and recombination. The final compositions and distributions of the clusters can provide more valuable information on the stability and bonding of clusters.

For generation of mixed clusters, the samples can be used in various ways. We have investigated transition metal/sulfur binary clusters by laser single ablation [11–13]. The laser single ablation only contains one target made of the mixture of transition metal and sulfur that is ablated by a laser beam. Kaya and co-workers applied laser ablation on two rotating targets to generate binary clusters [14]. Martin and co-workers used laser ablation on one sample and used an oven to vaporize another sample for the formation of mixed clusters of metal and fullerene [15]. More recently, we developed another laser ablation technique—laser double ablation (LDA) to generate mixed clusters [16]. The laser double ablation contains two separated targets that are ablated by laser beam, respectively. Here, we report on the Pb/S clusters produced from two different sources—the LSA and the LDA, respectively. The produced cluster ions were recorded by a tandem time-of-flight mass spectrometer (tandem TOF MS). The mass-selected cluster ions were further photolyzed and mass analyzed by the secondary stage of tandem TOF MS. Based on these experimental results, the differences in cluster formation in the LSA and LDA are discussed in this article.

2. Experimental

In the LSA, a well-mixed Pb + S sample was prepared by grinding the mixture of Pb (99.9%) and precipitated S (99%) into fine powder, and pressing it into a tablet with 12 mm diameter and 5 mm thickness to form the laser target. To examine the dependence of cluster distribution on the composition of solid sample, the molar ratio for Pb:S in the samples was varied from 1:1 to 1:8 in the experiments. The sample target was mounted in the source chamber of the tandem TOF MS, which was evacuated to 10^{-4} Pa before laser ablation. The laser ablation was carried out by the second harmonic of a pulsed Nd:YAG laser (532 nm wavelength, 10 ns pulse width, 10 Hz, 10–20 mJ/pulse). The laser beam was gently focused with a lens ($f = 50$ cm) to a spot of 0.5 mm diameter on the target with a power density on the order of 10^7 W/cm^2. The target surface under ablation was vaporized into a plume in a plasma state consisting of electrons, atoms, molecules, and other small species, either neutral or charged. Complicated reactions took place in the plasma [10], and Pb/S binary clusters were produced therein.

The LDA is conceptually the same technique as the LSA, with the difference being in the arrangement of laser targets [16]. As indicated in Fig. 1, two sample targets, pure Pb and pure S, were arranged in the LDA instead of a single mixed Pb + S target in the LSA. The two targets were placed parallel to each other and separated by a fixed distance, with the S target in front. A channel of 0.5 mm diameter was drilled throughout the S target, so the laser could pass through the channel and reach the surface of the Pb target. In such a setup, the laser can simultaneously ablate both S and Pb. If the distance between the two targets is too short, the emitted species from the two targets meet first and then the mixed clustering occurs. This clustering process is similar to that in the LSA as discussed above. But if the distance between targets is long enough for the accomplishment of

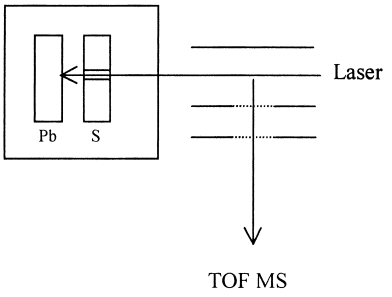

Fig. 1. Scheme of the LDA.

independent clustering of the emitted species from each target, then the reactions between two kinds of clusters can be achieved when some of the clusters from the first target sputter through the channel of the second target. In the latter case, the LDA can be used to study the reactions between clusters. This is, in fact, the main consideration in the development of LDA and the intrinsic feature of this setup. Compared with the Fourier transform ion cyclotron resonance mass spectrometer [17] and the flow tube reactor [18], which have been extensively applied in studies on reactions of clusters, the LDA is much simpler and still efficient.

The analysis of cluster ions was conducted by the homemade tandem TOF MS, the details of which were published elsewhere [19]. In brief, the cluster ions produced by laser ablation were extracted and accelerated by 0.1 kV and 1.1 kV, respectively, and entered the flight tube. After flying over a 3.5-m-long field-free flight tube, the clusters with different masses were separated and detected by the dual microchannel plates. The mass resolution of the first stage of tandem TOF MS is about 300. The cluster cations with a specific mass can be picked out by a mass gate at the end of the flight tube. The selected ions were then decelerated by a retarding field of 0.9 kV, and photolyzed by an excimer laser beam (Lambda Physik LPX 300, KrF, 248 nm wavelength, 4 ns pulse width, 10 Hz, 10 mJ/cm^2). Following laser radiation, both the remaining parent ions and the fragment ions were reaccelerated and then mass analyzed by the second stage of the tandem TOF MS, which was perpendicular to the first stage. The signals from either the first stage or the second stage were

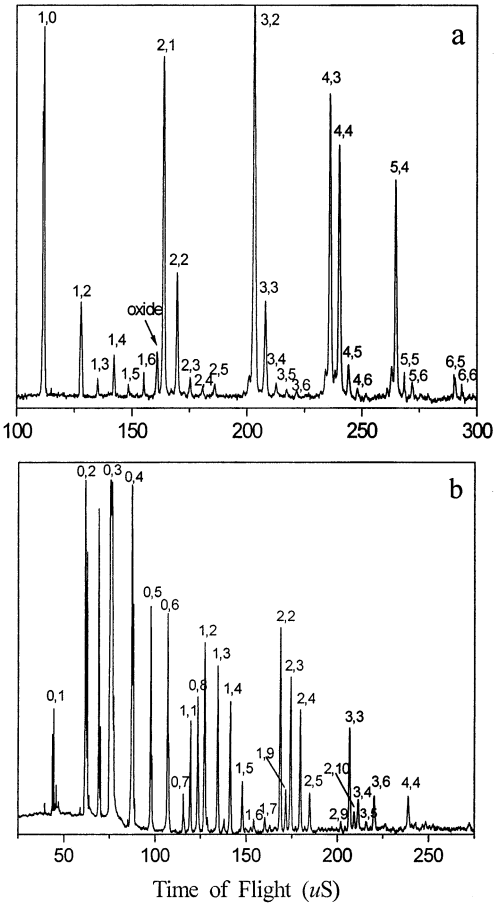

Fig. 2. TOF mass spectra of Pb/S cluster ions produced by LSA on a mixed sample with Pb:S = 1:4, (a) cations $Pb_nS_m^+$ and (b) anions $Pb_nS_m^-$.

recorded with a 10 MHz transient recorder, preamplified and stored in an IBM personal computer. For measurements, the digitized mass spectrum obtained in each laser shot was accumulated over 2000 shots.

3. Results

3.1. Pb/S binary cluster ions produced by the LSA

A typical TOF mass spectrum of Pb/S cluster cations produced by the LSA on a mixed sample with Pb:S = 1:4 is shown in Fig. 2(a). The mass peaks in the figure are labeled with (n, m), representing the number of Pb atoms (n) and S atoms (m) in cluster

ions. The cations can be divided into several groups according to the number of Pb atoms contained in clusters, and each group includes several species with the same number of Pb atoms and a various number of S atoms, such as PbS_m^+ ($m = 0$–6), $Pb_2S_m^+$ ($m = 1$–5), $Pb_3S_m^+$ ($m = 2$–6), $Pb_4S_m^+$ ($m = 3$–6), $Pb_5S_m^+$ ($m = 4$–6), and $Pb_6S_m^+$ ($m = 5$–6). The first interesting observation of the clusters is their size distribution. In each group of $Pb_nS_m^+$ with a fixed n, $Pb_nS_{n-1}^+$ is always at the outset of the group, followed by the satellite-like clusters $Pb_nS_m^+$ with $m \geq n$. In other words, no clusters of $Pb_nS_m^+$ with $m < n - 1$ appear in the group, and $Pb_nS_{n-1}^+$ is the most intense mass peak in the group, whereas the mass peaks of $Pb_nS_m^+$ with $m \leq n$ sharply drop down. In addition, there exists an odd–even oscillation of the intensities for PbS_m^+. The intensities of PbS_m^+ with $m = 0, 2, 4, 6$ are greater than those with $m = 1, 3, 5$.

These distribution patterns are completely independent of the composition of the sample ablated by laser. By decreasing the S content in a sample to a molar ratio of Pb:S = 1:1, the number of cluster ions are greatly diminished, but all the $Pb_nS_{n-1}^+$ including Pb^+, Pb_2S^+, $Pb_3S_2^+$, and $Pb_4S_3^+$ are still kept as prominent peaks in the mass spectra and no cluster ions with deficient S atoms (i.e. $m < n - 1$) appear, even under a very low S content in the sample. On the other hand, increasing the S content to a molar ratio of Pb:S = 1:8 in a sample can produce $Pb_nS_m^+$ with larger m, and the characteristics of cluster distribution mentioned in Fig. 2(a), including the domination of $Pb_nS_{n-1}^+$ and the odd/even effect in PbS_m^+ intensities, remain unchanged in this case.

The anion spectrum of Pb/S clusters contains pure sulfur cluster anions and binary anions, as shown in Fig. 2(b). The binary anion compositions can be expressed as $Pb_nS_m^-$ with $m \geq n$. In each group of $Pb_nS_m^-$ with a fixed n, no species with deficient S atoms (i.e. $m < n$) are presented. Also, $Pb_nS_n^-$ is the most abundant cluster ion in each group. Compared with Pb/S cluster cations, the intensity of the Pb/S cluster anions also varies with the relative content of Pb and S in a sample, but the prominence of the cluster anions $Pb_nS_n^-$ in the mass spectrum as well as the relation of $m \geq n$ is not affected by the variation of sample composition.

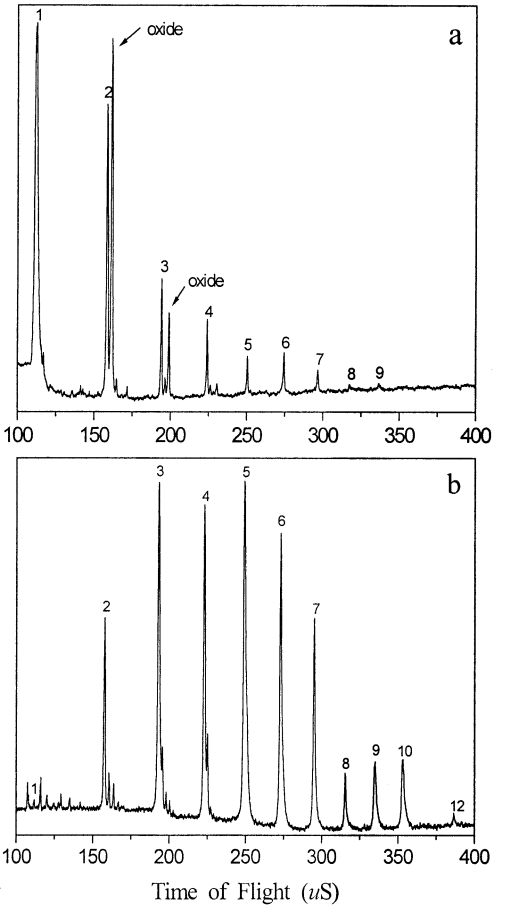

Fig. 3. TOF mass spectra of Pb cluster ions produced by laser ablation on a Pb sample, (a) cations Pb_n^+ and (b) anions Pb_n^-.

3.2. Pb/S binary cluster ions produced by the LDA

To study the reactions between Pb clusters and S clusters, the prerequisite is the independent clustering of Pb and S. It is known that Pb and S are apt to form mono clusters, respectively [20–22]. The S_n clusters can be formed up to $n = 10$ by laser ablation of pure S [22]. The clustering of Pb has also been verified in the present experiment. Fig. 3 illustrates the mass spectra of the cations and anions of Pb clusters by laser ablation of pure Pb. Pb cluster ions can be formed up to Pb_9^+ and Pb_{12}^-. The Pb_n anions exceed

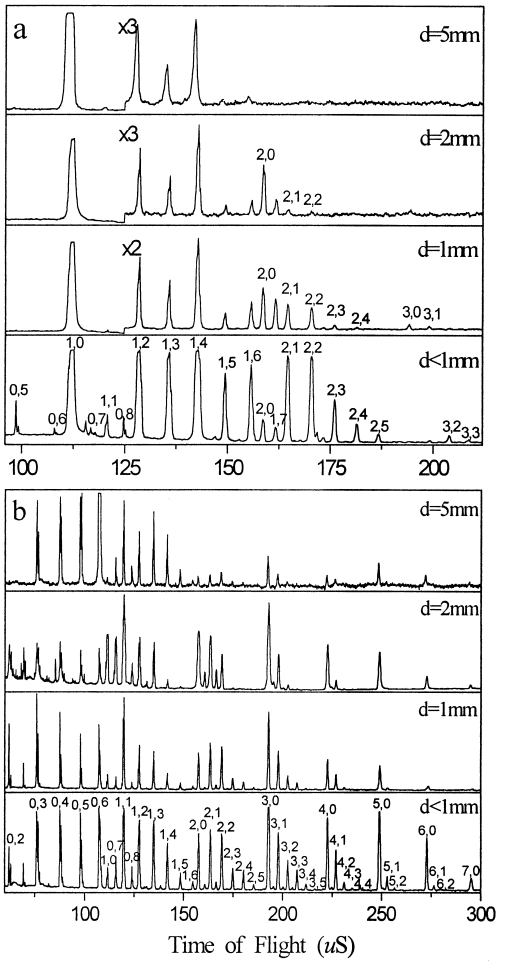

Fig. 4. TOF mass spectra of Pb/S cluster ions produced by LDA on separated Pb and S with different distances between two targets, (a) cations $Pb_nS_m^+$ and (b) anions $Pb_nS_m^-$.

the cations in size, and the intensity distributions of cations and anions are rather different. This means that the total number of valence electrons in Pb clusters, rather than the geometrical structure, influences the stability of Pb clusters. Thus, from the results above, the reactions between Pb clusters and S clusters can be expected by LDA.

Fig. 4 shows the reaction products generated by LDA, in which "d" represents the distance between two targets. In experiments, the dependence of product distribution on the distance was carefully examined. When the distance is too large, the amount of products will decrease too much to be detected. The shorter the distance becomes, the more the products are detected. The products generated by LDA are summarized in Table 1. Generally, the cationic products $Pb_nS_m^+$ are in the range of $n = 0–3$ and $m = 0–7$, and the value of m declines when n increases in the $Pb_nS_m^+$. It is noted that the clusters PbS_m^+ ($m = 0–7$) produced by LDA also exhibit an odd–even alternation in intensities with the m values. The PbS_m^+ with even m are more intense than the neighboring with odd m, like the same PbS_m^+ clusters produced by LSA.

The anionic products $Pb_nS_m^-$ are more abundant than the cationic products $Pb_nS_m^+$, and the size of the anions n can range from 0–7 and m from 0–9. The richer array of anionic products may be attributed to the facile formation of anionic S clusters and/or Pb clusters because electron affinity of neutral leading to anions is more energy favored than ionization of neutral leading to cations. In each group of $Pb_nS_m^-$ with a fixed n, the pure Pb_n^- has maximum intensity and the intensities of $Pb_nS_m^-$ decline smoothly with increasing m.

3.3. UV photodissociation of Pb/S cluster ions

By mass selection, a function of the tandem TOF MS, the experiments on photodissociation of cluster cations were performed with a 248 nm laser. Fig. 5 is a typical mass spectrum obtained from the photodissociation of $Pb_4S_4^+$. As shown, there exist five photodissociation channels leading to Pb^+, Pb_2^+, Pb_2S^+, $Pb_2S_2^+$, and $Pb_3S_2^+$, respectively. From the relative intensity of these fragment ions, we can estimate the efficiency R_j of each photodissociation channel according to Eq. (1),

$$R_j = I_j \Big/ \sum_i I_i \tag{1}$$

where I_j is the intensity of the studied fragment ion and $\sum_i I_i$ is the sum of intensities including all fragment ions and the remaining parent ion.

In order to compare the properties of the clusters produced by LSA and LDA respectively, cluster cations with the same composition but produced in different sources were studied by photodissociation. Table 2 summarizes the photodissociation channels

Table 1
The distributions of ionic products in the LDA with different distances between two targets

Distance/mm	Cations $Pb_nS_m^+$	Anions $Pb_nS_m^-$	
<1	$n = 0$, $m = 1$–8	$n = 0$, $m = 1$–8	$n = 1$, $m = 0$–8
	$n = 1$, $m = 0 \sim 7$	$n = 2$, $m = 0$–5, 7–9	$n = 3$, $m = 0$–7
	$n = 2$, $m = 0 \sim 5$	$n = 4$, $m = 0$–4	$n = 5$, $m = 0$–2
	$n = 3$, $m = 0 \sim 3$	$n = 6$, $m = 0$–2	$n = 7$, $m = 0$
1	$n = 1$, $m = 0 \sim 7$	$n = 0$, $m = 1$–8	$n = 1$, $m = 0$–8
	$n = 2$, $m = 0 \sim 4$	$n = 2$, $m = 0$–5	$n = 3$, $m = 0$–4
	$n = 3$, $m = 0 \sim 1$	$n = 4$, $m = 0$–2	$n = 5$, $m = 0$–1
		$n = 6$–7, $m = 0$	
2	$n = 1$, $m = 0 \sim 7$	$n = 0$, $m = 1$–8	$n = 1$, $m = 0$–5
	$n = 2$, $m = 0 \sim 2$	$n = 2$, $m = 0$–3	$n = 3$, $m = 0$–2
		$n = 4$–5, $m = 0$–1	$n = 6$–7, $m = 0$
5	$n = 1$, $m = 0 \sim 6$	$n = 0$, $m = 0$–8	$n = 1$, $m = 0$–6
		$n = 2$, $m = 0$–3	$n = 3$, $m = 0$–2
		$n = 4$, $m = 0$–1	$n = 5$–7, $m = 0$

and the corresponding efficiencies for each cation. The photodissociation of cluster cations larger than $Pb_2S_5^+$ produced by LDA cannot be carried out because of their weak intensities.

4. Discussion

4.1. Formation pathway of Pb/S binary clusters in the LSA

In the analysis of the mass spectra of cluster ions, we often pay attention to those mass peaks that always have high intensities independent of sample composition. As stated in many researches of binary clusters [11–13,23–24], such peaks can be defined as the stable compositions of binary clusters and usually correspond to high stable structures. With regard to the Pb/S system, it can be confirmed that $Pb_nS_{n-1}^+$ and $Pb_nS_n^-$ are formed preferentially, relative to other stoichiometries, thus they can be defined as the stable compositions of the Pb/S cluster ions. All produced cluster ions can be included as $Pb_nS_m^+$ ($m \geq n$) and $Pb_nS_m^-$ ($m \geq n - 1$); and specifically, no clusters with deficient S atoms (i.e. $Pb_nS_m^+$ with $m < n$ and $Pb_nS_m^-$ with $m < n - 1$) appear. So it is reasonable to think that the $Pb_nS_{n-1}^+$ and $Pb_nS_n^-$ construct the skeletons of Pb/S binary clusters and are formed first during the clustering, and then the extra S atoms (the number of which depends on the S content in samples) attach to the skeletons as ligands.

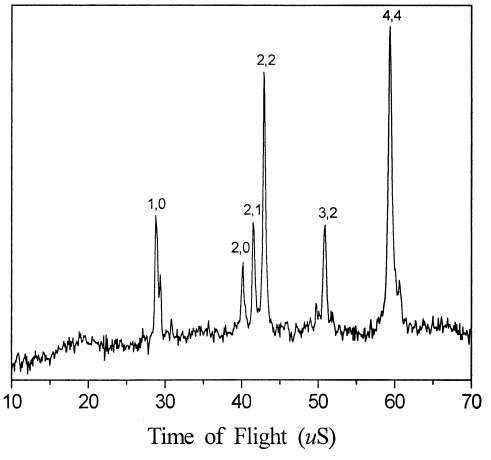

Fig. 5. Second-stage TOF mass spectrum of the fragment ions of $Pb_4S_4^+$ when photolyzed at the 248 nm laser.

The odd–even alternation in intensities of PbS_m^+ provides the details of cluster formation. It is known that the S_2 molecule dominates in the sulfur vapor from 600 K to 2500 K in a very wide pressure range [25], thus the PbS_m^+ may be mainly constructed by successive bonding of S_2 to Pb^+ or to PbS^+. Because of the high reactivity of the term-coordinated S atom in PbS^+, it is unstable and easy to dissociate or combine with other species [26]. Therefore, the PbS_3^+, PbS_5^+ clusters resulting from the precursor PbS^+ are fewer than PbS_2^+, PbS_4^+, and PbS_6^+ resulting from the precursor Pb^+. It has been

Table 2
Photodissociation of Pb/S cluster cations produced by LSA (column I) and LDA (column II)

Parent ions	Dissociation channel	I		II		Parent ions	Dissociation channel	I	
		R_i	ΣR_i	R_i	ΣR_i			R_i	ΣR_i
PbS_2^+	$PbS^+ + (S)$	0.09		0.06		$Pb_2S_8^+$	$Pb_2S^+ + (S_7)$	0.15	
	$Pb^+ + (S_2)$	0.18	0.31	0.24	0.30		$Pb_2^+ + (S_8)$	0.12	0.51
	$S^+ + (PbS)$	0.04		0			$Pb^+ + (PbS_8)$	0.24	
PbS_3^+	$PbS^+ + (S_2)$	0.08		0.03		$Pb_3S_2^+$	$Pb_2S^+ + (PbS)$	0.07	
	$Pb^+ + (S_3)$	0.11	0.19	0.11	0.14		$Pb^+ + (Pb_2S_2)$	0.45	0.52
PbS_4^+	$PbS^+ + (S_3)$	0		0.02		$Pb_3S_3^+$	$Pb_2S^+ + (PbS_2)$	0.27	
	$Pb^+ + (S_4)$	0.22	0.22	0.30	0.32		$Pb_2^+ + (PbS_3)$	0.06	0.39
							$Pb^+ + (Pb_2S_3)$	0.06	
PbS_5^+	$PbS_2^+ + (S_3)$			0.09					
	$PbS^+ + (S_4)$			0.22	0.42	$Pb_3S_4^+$	$Pb_2S^+ + (PbS_3)$	0.40	
	$Pb^+ + (S_5)$			0.11			$Pb_2^+ + (PbS_4)$	0.05	0.62
							$Pb^+ + (Pb_2S_4)$	0.17	
PbS_6^+	$PbS_2^+ + (S_4)$	0.06		0.35					
	$PbS^+ + (S_5)$	0.13	0.58	0.04	0.69	$Pb_3S_5^+$	$Pb_2S_2^+ + (PbS_3)$	0.47	
	$Pb^+ + (S_6)$	0.39		0.30			$Pb_2S^+ + (PbS_4)$	0.06	0.61
							$Pb_2^+ + (PbS_5)$	0.04	
Pb_2S^+	$Pb_2^+ + (S)$	0.15		0.05					
	$PbS^+ + (Pb)$	0.08	0.28	0.03	0.15		$Pb^+ + (Pb_2S_5)$	0.04	
	$Pb^+ + (PbS)$	0.05		0.07					
						$Pb_3S_6^+$	$Pb_3S_2^+ + (S_4)$	0.21	
$Pb_2S_2^+$	$Pb_2S^+ + (S)$	0.07		0			$Pb_2S_2^+ + (PbS_4)$	0.08	
	$Pb_2^+ + (S_2)$	0.22	0.28	0.06	0.20		$Pb_2S^+ + (PbS_5)$	0.13	0.59
	$Pb^+ + (PbS_2)$	0		0.14			$Pb_2^+ + (PbS_6)$	0.04	
							$Pb^+ + (Pb_2S_6)$	0.13	
$Pb_2S_3^+$	$Pb_2S^+ + (S_2)$	0.04		0					
	$PbS^+ + (PbS_2)$	0.04		0.08		$Pb_4S_3^+$	$Pb_2S^+ + (Pb_2S_2)$	0.43	
	$PbS_2^+ + (PbS)$	0	0.48	0.04	0.58		$Pb_2^+ + (Pb_2S_3)$	0.05	0.48
	$Pb^+ + (PbS_3)$	0.4		0.46		$Pb_4S_4^+$	$Pb_3S_2^+ + (PbS_2)$	0.11	
							$Pb_2S_2^+ + (Pb_2S_2)$	0.23	
$Pb_2S_4^+$	$Pb_2S^+ + (S_3)$	0.06		0.06					
	$Pb_2^+ + (S_4)$	0.06		0.09			$Pb_2S^+ + (Pb_2S_3)$	0.08	0.63
	$PbS_2^+ + (PbS_2)$	0.09	0.47	0.10	0.57		$Pb_2^+ + (Pb_2S_4)$	0.06	
	$PbS^+ + (PbS_3)$	0.06		0.08			$Pb^+ + (Pb_3S_4)$	0.15	
	$Pb^+ + (PbS_4)$	0.2		0.24					
						$Pb_5S_4^+$	$Pb_3S_3^+ + (Pb_2S)$	0.07	
$Pb_2S_5^+$	$Pb_2S^+ + (S_4)$	0.26		0.25			$Pb_3S_2^+ + (Pb_2S_2)$	0.57	
	$Pb_2^+ + (S_5)$	0.18		0.04			$Pb_3S^+ + (Pb_2S_3)$	0.02	0.95
	$PbS_2^+ + (PbS_3)$	0	0.56	0.05	0.39		$Pb_2^+ + (Pb_3S_4)$	0.22	
	$PbS^+ + (PbS_4)$	0		0.01			$PbS^+ + (Pb_4S_3)$	0.05	
	$Pb^+ + (PbS_5)$	0.12		0.04			$Pb^+ + (Pb_4S_4)$	0.02	

shown that the clusters PbS_m^+ were photodissociated to give Pb^+ and PbS^+ as main products, which is consistent with the precursors Pb^+ and PbS^+.

The formation of clusters produced by LSA is somewhat different from that of Saito et al. [9]. In their study, the main cluster cations were not $Pb_nS_{n-1}^+$ but $Pb_nS_n^+$, and also the cluster cations with deficient S atoms (i.e. $Pb_nS_m^+$ with $m < n - 1$) were produced with higher intensity than those with excess S atoms. The following is a typical intensity distribution of the clusters $Pb_2S_m^+$ in their article: $Pb_2S_2^+ > Pb_2^+ \sim Pb_2S^+ > Pb_2S_3^+ > Pb_2S_4^+$, which is different from the sequence of $Pb_2S^+ \gg Pb_2S_2^+ > Pb_2S_3^+ > Pb_2S_4^+ > Pb_2S_5^+$, shown in the present study. This discrepancy is not surprising if one considers the different clustering conditions in the two studies. In Saito's experi-

ment, the clusters were generated by condensation of the vapor of a PbS compound in the expanding nozzle flow and ionized by electron bombardment. In this process the precursor PbS molecule remained as the main species to form clusters. On the other hand, in our experiment, the atoms of Pb and S were vaporized into plasma and the cluster ions were produced directly. In other words, no precursor like PbS existed in our experiment. The different cluster distributions in these two studies support the idea that the formation and distribution of clusters depend greatly on the experimental conditions. In addition, the flight time of cluster ions indicated in the TOF mass spectra in Saito's article was about 25–75 μS; this observation time is much shorter than that of 100–400 μS in our experiment. It is reasonable that the difference in cluster ion intensities between Saito's and ours can be partially attributed to the different time scales of the experiments.

4.2. Formation pathway of Pb/S binary clusters in the LDA

It has been shown that when the Pb target and S target were compactly arranged with $d < 1$ mm, the resulting cationic cluster mass spectrum was very similar to that in the LSA, with $Pb_nS_m^+$ ($m \geq n - 1$) as main products. This means that the formation scheme derived from the LSA can also be applied in this case. However, when the two targets were separated with $d \geq 1$ mm, the results were quite different. The most intense peaks are assigned to pure Pb_n clusters such as Pb^+, Pb_2^+, and Pb_3^+, followed by the binary clusters $Pb_nS_m^+$ with $m \geq 1$. The difference between the LSA and LDA becomes more distinct for anionic clusters. With LSA, the main clusters are $Pb_nS_m^-$ with $m \geq n$; whereas with LDA, at each distance, the mass spectra are dominated by Pb_n^- ions ($n = 1$–7) and $Pb_nS_m^-$ with deficient S atoms ($m < n$). In a word, both the composition and distribution of cluster ions obtained by LDA and LSA are quite different.

How are these clusters with deficient S atoms generated in the LDA? For the answer, two possible origins are proposed. One is from the fragmentation of larger clusters with excess S atoms, and another is from the attachment of S atoms directly to pure Pb_n clusters. However, if the former origin is a main channel, the $Pb_nS_m^+$ with $m < n - 1$, the $Pb_nS_m^-$ with $m < n$, and pure $Pb_n^\pm$ should be observed in the LSA, but it was not true in our experiment. It is conceivable, therefore, that the latter origin is more favored. Specifically, with LDA, the Pb clusters are formed first, and then they react with sulfur to produce binary clusters. The fact that pure Pb_n clusters were not observed in the mass spectra produced by LSA indicates that there is competition between the clustering of Pb with S and that of Pb with Pb, and the former overwhelms the latter. Thus in order to study the reaction of a Pb cluster with sulfur, the clustering of Pb itself must be completed prior to the reaction with sulfur, which can be achieved by tuning the distance between two targets in the LDA experiment. The pure Pb_n^+ and cationic reaction products $Pb_nS_m^+$ ($m < n - 1$) were not observed in the LDA when the distance was too short (e.g. Fig. 4(a), $d < 1$ mm), due to clustering of Pb and S rather than the reaction of the Pb cluster with S. On the other hand, the reaction products of the Pb cluster and S decreased greatly at larger distances, although the pure Pb_n clusters had sufficient intensity (e.g. Fig. 4(b), $d = 2$ mm). This tendency may be attributed to the decrease in collisions leading to the reaction of the Pb cluster with S in the cooled plume. Furthermore, the distinct size effect was observed in the reaction of Pb clusters with sulfur: the larger the Pb cluster becomes, the fewer S atoms the cluster combines.

4.3. Stability of Pb/S binary cluster ions

Mass-selected photodissociation can provide information on formation and stability of clusters. As listed in Table 2, for clusters PbS_m^+ produced by LSA and LDA, the channels and efficiencies of photodissociation are almost identical. The general agreement and the same odd–even alternation in intensity reveal that the clusters PbS_m^+, independent of the origins of generation, have the same stability pattern. Actually, all the PbS_m^+ ions come from the same formation—reaction of one Pb atom and several S atoms in either source—with the stable PbS_m^+ ions coming from the combination of one Pb and even S atoms. However,

when Pb atoms in parent $Pb_nS_m^+$ ions are larger than one, the situation seems to be somewhat different. For example, either the photodissociation channels or the photodissociation efficiency of $Pb_2S_2^+$, $Pb_2S_3^+$, and $Pb_2S_5^+$ generated by LSA and LDA, respectively, are different, which shows that the cluster ions $Pb_nS_m^+$ ($n > 1$) produced by LSA are different from that produced by LDA in properties and/or structure. For small clusters, such differences can be related to different internal energy because they are formed at different temperatures from the two sources. The different internal energy then leads to different absorption cross sections and thus different degrees of photofragmentation. But for larger clusters containing more than three Pb atoms, the different source can indeed produce structural isomers of the same composition.

Focusing on the clusters generated by LSA, their photodissociation can be concluded as follows: (1) When the number of S atoms is much larger than that of Pb atoms, the loss of S atoms is a common process during photodissociation, such as the loss of S_4, S_5, and S_6 from PbS_6^+, and the loss of S_7 from $Pb_2S_8^+$. The kicked-out S atoms are probably loosely attached as ligands to the skeleton of clusters. (2) The main charged fragments still have the compositions of $Pb_nS_{n-1}^+$, such as Pb^+, Pb_2S^+, and $Pb_3S_2^+$, confirming the high stability of the $Pb_nS_{n-1}^+$. In addition, the experiments show that $Pb_2S_2^+$ is another main fragment of $Pb_3S_5^+$, $Pb_3S_6^+$, and $Pb_4S_4^+$, indicating that $Pb_2S_2^+$ is stable. (3) For all clusters with the stable compositions $Pb_nS_{n-1}^+$, also called the skeletons of clusters, the most efficient fragmentation is the neutral loss of Pb_2S_2, as shown in Table 2. Although the real state of neutral Pb_2S_2 fragments cannot be determined in the present experiment, there does exist the possibility that Pb_2S_2 may probably appear as a square unit.

It is generally believed that negative cluster ions are formed by the attachment of low energy electrons to neutral species in plasma, and are more similar to neutral species in stability than positive ones. Thus the stoichiometry similarity between the most intense $Pb_nS_n^-$, the second most intense $Pb_nS_n^+$ obtained in our experiment, and the $Pb_nS_n^+$ obtained by Saito [9] should imply the high stability of neutral Pb_nS_n. Particularly, it is seen that both $Pb_4S_4^+$ and $Pb_4S_4^-$ stand out as intense

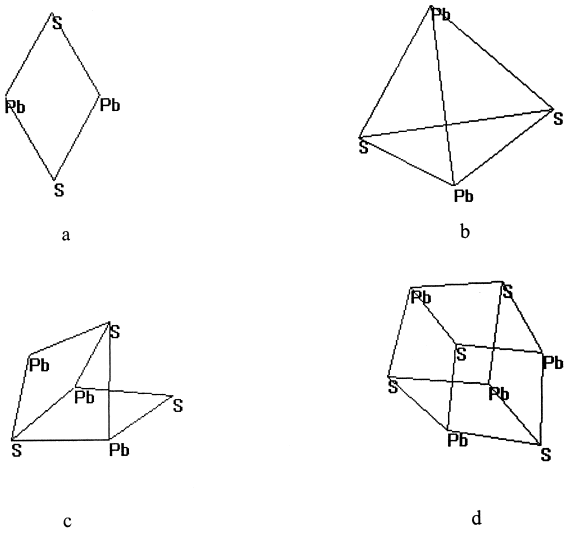

Fig. 6. Possible structures of (a), (b) Pb_2S_2, (c) Pb_3S_3, and (d) Pb_4S_4.

peaks in Fig. 2(a) and (b). This consistency suggests that the neutral Pb_4S_4 must be very stable, thus losing or gaining an electron will not affect its stability.

The structural models of some neutral Pb_nS_n clusters are proposed from these results. Fig. 6 shows the structural evolution from Pb_2S_2 to Pb_4S_4 that has been optimized by the MM+ molecular dynamic methods. For Pb_2S_2 there may exist two possible structures: a planar rhombic unit with a weak Pb–Pb bond (a) and a tetrahedron (b), but the rhombic configuration is more favored in molecular dynamics and MNDO geometry optimization. The MNDO energy of the (a) structure is −522.18647 eV, lower than that of the (b) structure (−521.24501 eV). For Pb_4S_4, the high stability might be attributed to a possible stable cube-like configuration (d). This structure is the combination of two Pb_2S_2 units. Each S atom simultaneously bonds to three Pb atoms, and each Pb atom also simultaneously bonds to three S atoms, corresponding to a segment of bulk PbS lattices [27]. And for Pb_3S_3, a structure (c) between Pb_2S_2 and Pb_4S_4 is proposed with two μ3-bridging S atoms and one μ2-bridging S atom. As shown in Fig. 6, the PbS clusters are inclined to form closo-structures with a Pb–S bond, and approach the structure of the bulk PbS compound as clusters grow. Particularly, the

structure of Pb_4S_4 is the same as the face central cube (fcc) lattice of lead sulfide crystals. Such structural similarity between the clusters and bulk material have been found in many binary systems before, e.g. the calculated structural forms of $(NaCl)_n$ and $Na(NaCl)_n^+$ are all cube-like [28]. This suggests the intrinsic relation between bonds and structures as well as the transition from clusters to bulk compounds.

The structure of Pb_2S^+ can be achieved by removing an S atom in (a), but the remaining $[Pb–S–Pb]^+$ will change to a linear configuration as calculated by MNDO. The structure of $Pb_3S_2^+$ is proposed as a trigonal bipyramid by removing one S atom in (c), and the two remaining S atoms cap the Pb_3 triangle. Elimination of any one S vertex from (d) will yield the structure of $Pb_4S_3^+$. These proposed cation structures are in agreement with the observed fragmentation models, and more precise theoretical calculations by B3LYP/LANL2DZ are under way.

5. Conclusions

Pb/S binary cluster ions have been produced by LSA and LDA, and some of them were photolyzed by UV laser. Through LSA on a mixed Pb + S sample, the stable compositions $Pb_nS_{n-1}^+$ and $Pb_nS_n^-$ are formed as structural skeletons in the construction of Pb/S binary cluster ions, and they have a high stability that is also confirmed in the photodissociation of clusters. The structural models of these clusters are proposed. In LDA on separated Pb sample and S sample, Pb clusters and S clusters are generated individually first, then the reactions between Pb clusters and S clusters occur to produce binary clusters. The compositions as well as the abundance of the cluster species produced in the LSA and LDA are quite different. Although the cluster ions have the same compositions, they may have different internal energy or structure depending on the way in which they were produced. Such observations suggest that the investigation of cluster chemistry must be traced back to the formation process of the cluster.

Acknowledgement

This work was supported by the Natural Science Foundation of China.

References

[1] H. Hinterberger, Z. Physik. 119 (1942) 1.
[2] R.S. Kane, R.E. Cohen, R. Silbey, J. Phy. Chem. 100 (1996) 7928.
[3] A. Henglein, Chem. Rev. 89 (1989) 1861.
[4] Y. Wang, A. Suna, W. Mahler, R. Kasowski, J. Chem. Phys. 87 (1987) 7315.
[5] Y. Wang, Acc. Chem. Res. 24 (1991) 133.
[6] Y. Wang, N. Herron, J. Phys. Chem. 91 (1987) 257.
[7] R.S. Kane, R.E. Cohen, R. Silbey, Chem. Mater. 8 (1996) 1919.
[8] R. Colin, J. Drowart, J. Chem. Phys. 37 (1962) 1120.
[9] Y. Saito, K. Mihama, T. Noda, Jpn. J. Appl. Phys. 22 (1983) L179.
[10] M.L. Mandich, W.D. Reents, V.E. Bondybey, in E.R. Bernstein (Ed.), Atomic and Molecular Clusters, Elsevier, Amsterdam, 1990, Chap. 2.
[11] Y. Shi, Z.D. Yu, N. Zhang, Z. Gao, F.A. Kong, Q.H. Zhu, J. Chin. Chem. Soc. 42 (1995) 455.
[12] Z.D. Yu, N. Zhang, X.J. Wu, Z. Gao, Q.H. Zhu, F.A. Kong, J. Chem. Phys. 99 (1993) 1765.
[13] Y. Shi, N. Zhang, Z. Gao, F.A. Kong, Q.H. Zhu, J. Chem. Phys. 101 (1994) 1.
[14] K. Kaya, Kenkyu Hokoku-Asahi Garaus Zaidan (Japan) 58 (1991) 253.
[15] W. Branz, I.M.L. Billas, N. Malinowski, F. Tast, M. Heinebrodt, T.P. Martin, J. Chem. Phys. 109 (1998) 3425.
[16] Z. Gao, P. Liu, Rev. Sci. Instrum. 69 (1998) 1837.
[17] K.J. Fisher, I.G. Dance, G.D. Willett, Rapid Commun. Mass Spectrom. 10 (1996) 106.
[18] D.M. Cox, A. Kaldor, P. Fayet, W. Eberhardt, R. Brickman, R. Sherwood, Z. Fu, D. Sodericher, ACS Symp. Ser. 173 (1990) 437.
[19] Z. Gao, F.A. Kong, X.J. Wu, N. Zhang, Q.H. Zhu, Z.P. Zhang, Q.Z. Liu, Chin. J. Chem. Phys. 5 (1992) 343.
[20] K. LaiHing, R.G. Wheeler, W.L. Wilson, M.A. Duncan, J. Chem. Phys. 87 (1987) 3401.
[21] I. Katakuse, T. Ichihara, H. Ito, Int. J. Mass Spectrom. Ion Processes 91 (1989) 93.
[22] N. Zhang, Z. Gao, F.A. Kong, Q.H. Zhu, L.S. Zheng, R.B. Huang, Prog. Nat. Sci. (China) 3 (1993) 170.
[23] T.P. Martin, J. Chem. Phys. 83 (1985) 78.
[24] X.H. Liu, X.G. Zhang, Y. Li, X.Y. Wang, N.Q. Lou, Int. J. Mass Spectrom. Ion Processes 177 (1998) L1.
[25] J. Berkowitz, in B. Meyer (Ed.), Element Sulfur, Chemistry and Physics, Interscience, New York, 1965, Chap. 23.
[26] X.T. Wu, Q. Huang, Q.M. Wang, T.L. Sheng, J.X. Lu, ACS Symp. Ser. 653 (1996) 282.
[27] (a) B. Wasserstin, Am. Mineral. 36 (1951) 102.
[28] T.P. Martin, in Clusters of Atoms and Molecules I, H. Haberland (Ed.), Springer-Verlag, Berlin, 1995, p. 363.